



# Role of the dipole mode index in governing the freshwater content within the bay of bengal summer pycnocline

Shannon M. Bohman<sup>\*</sup>, Arnold L. Gordon

Lamont-Doherty Earth Observatory of Columbia University, Palisades, NY, 10964, USA

## ABSTRACT

The Bay of Bengal (BoB) surface layer receives approximately  $0.13 \text{ million m}^3/\text{sec}$  ( $0.13 \text{ Sv}$ ) of freshwater through a combination of precipitation and river runoff minus evaporation, which then is exported to neighboring seas. Quasi-stationary salinity is established by the import of salty water from the Arabian Sea (AS), primarily within the pycnocline as an estuarine type of circulation. The BoB pycnocline is also affected by low salinity export from the southern Andaman Sea (AndS). We use Argo observations and GODAS reanalysis products to trace the spreading of AS and AndS water within BoB pycnocline during the summer monsoon when the bulk of AS water is imported. We use relative freshwater content (RWC), which is zero for pure AS water and 1 for pure AndS water. We find significant interannual variability of the RWC pattern, which relates to the Indian Ocean Dipole, as defined by the Dipole Mode Index (DMI). The position of the Sri Lanka Dome (SLD) off the east coast of Sri Lanka varies with DMI: the SLD is farther east during negative DMI, which directs the AS water farther to the east in BoB; whereas during the positive DMI, the AS water is directed to the north.

## 1. Introduction

The surface layer of the Bay of Bengal (BoB) receives an immense amount of freshwater. The combined annual precipitation and river runoff minus evaporation ( $P + R-E$ ) for the BoB is  $+0.13 \text{ Sv}$ , inducing low sea surface salinity (SSS). West of India, the Arabian Sea (AS) is in sharp contrast to BoB. With the removal of freshwater,  $P + R-E$  of the AS is  $-0.11 \text{ Sv}$ , inducing SSS  $>3 \text{ ppt}$  above that of the BoB (Gordon et al., 2019). Additionally, the AS pycnocline receives salty inflow from the Persian Gulf and the Red Sea. The low salinity surface layer within BoB forms a barrier layer inhibiting vertical mixing (Jampana et al., 2019), resulting in a pycnocline reflective of inflow from neighboring seas. Notable is the salinity maximum near 100 m, drawn from the AS pycnocline via the southern rim of Sri Lanka, predominately during the summer monsoon (Gordon et al., 2016; Hormann et al., 2019).

In addition to the salty AS water spreading within the BoB pycnocline, low salinity water derived from the Andaman Sea (AndS) spreads westward into the BoB through three gaps in the Andaman archipelago (Fig. 1). The AndS, with a SSS of near  $31 \text{ psu}$ , receives freshwater inflow from rivers, notably the Irrawaddy River (Varkey et al., 1996; Chatterjee et al., 2017). Inflow from the  $\sim 900 \text{ km}$  long Strait of Malacca links the AndS to the South China Sea. The Malacca Strait is about  $30 \text{ m}$  deep and  $35 \text{ km}$  wide, deepening to  $\sim 100 \text{ m}$  at the AndS (Wyrtki, 1961). Wibowo et al. (2022) found that surface currents within the Strait of Malacca have an average current speed of  $\sim 0.13 \text{ m/s}$  towards the AndS during

the winter months, weakening to  $\sim 0.003 \text{ m/s}$  in summer. Important attributes of the AndS are strong tides and solitons boosting downward mixing of the low salinity surface layer into the pycnocline and deep water, which then spreads westward through a few channels into the BoB pycnocline, countering the salty AS input (Osborne and Burch, 1980; Jithin et al., 2020).

Hormann et al. (2019), using sea surface drifters, find two pathways through which low salinity surface layer of the Bay of Bengal (BoB) is exported into the tropical Indian Ocean and AS. The western route is located along the east coast of India and feeds into the westward Northeast Monsoon Current (NMC) around the southern rim of Sri Lanka during the winter monsoon. Relatively saline AS surface water is injected into BoB by the eastward flowing Summer Monsoon Current (SMC) around the southern rim of Sri Lanka. An eastern path for year-round export of BoB low salinity surface layer is located along the western margin of Sumatra. Herron et al. (2022) found that eddies are the dominant factor in exporting freshwater mainly in the upper  $\sim 50 \text{ m}$ , within the central BoB.

Cullen and Shroyer (2019) detail the interannual variability of the Sri Lanka Dome (SLD), an upwelling feature with cyclonic circulation occurring during the summer monsoon, east of Sri Lanka. The SLD acts as a gatekeeper directing the AS water injected in the BoB pycnocline into the interior of BoB. The SLD position and size is directly related to the local wind stress curl east of Sri Lanka, which is closely related to the Indian Ocean Dipole (IOD). The IOD, characterized by large-scale sea

<sup>\*</sup> Corresponding author.

E-mail address: [smb2317@columbia.edu](mailto:smb2317@columbia.edu) (S.M. Bohman).

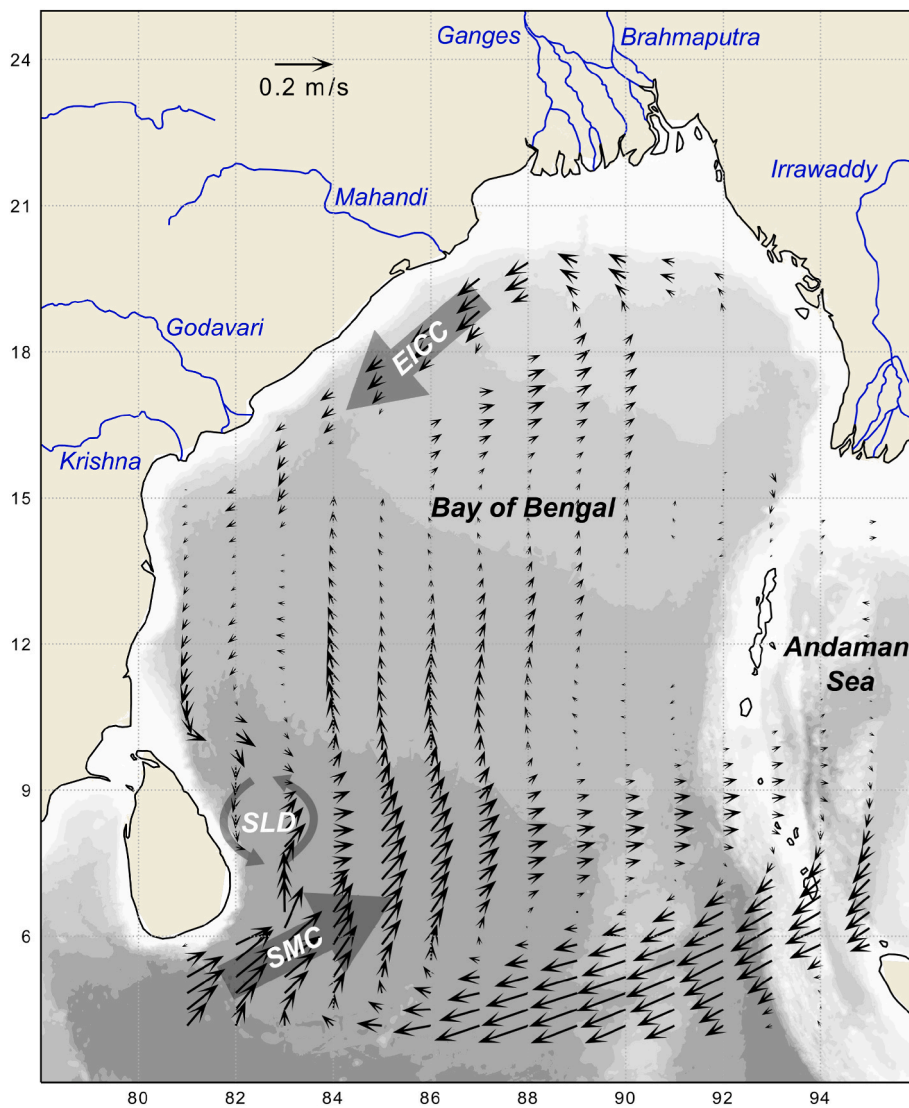


**Fig. 1.** Summer climatology (June–September 2004–2021) of GODAS currents within the 75–100 m depth interval. Gray contours show bathymetry. This climatology highlights the major circulation features we will be analyzing, including the SLD as cyclonic flow in the southwest, SMC as eastward flow in the southwest, and EICC as southward flow in the northwest.

surface temperature anomaly patterns in the tropical Indian Ocean, is a primary forcing mechanism driving interannual variability in the summer monsoon. El Niño Southern Oscillation (ENSO) is linked to the IOD (Meyers et al., 2007). While positive IOD events have been found to offset the effects of El Niño events, model studies find that ENSO events do not necessarily enhance the strength of the IOD (Ashok et al., 2004; McKenna et al., 2020).

Using Argo profiles, we investigate the spatial pattern and interannual variability of the relative freshwater content (RFWC), which is zero for pure AS water (salty end member; Fig. 2b) and 1 for the AndS water (fresh end member; Fig. 2b), during the summer monsoon when AS water injects salt into the BoB pycnocline (75–100 m depth slab; Fig. 2c). Our goal in this paper is to determine the relationship between the IOD, quantified by the Dipole Mode Index (DMI), and the spatial distribution of salty and fresh end members in the BoB pycnocline.

## 2. Data and methods

The study region within the BoB is 4–20°N and 80–96°E. Temperature and salinity observations were retrieved from the International Argo Program and the national programs that contribute to it (<https://argo.ucsd.edu>, <https://www.ocean-ops.org>).

The Argo Program is part of the Global Ocean Observing System. Since 1999, it has collected and made freely available over two million vertical temperature and salinity profiles around the world which, after quality control adjustments, are accurate to 0.002 °C for temperature, 2.4 dbar for pressure, and 0.01 PSS-78 for salinity (Wong et al., 2020).

We selected Argo profiles with at least 20 measurements between 10 and 300 m for the summer period, June through September 2004–2021. There were 3892 profiles that met these criteria within the study region. We highlight profiles representative of the AS (Fig. 2a, red profile; Fig. 2c, red X) and AndS (Fig. 2a, blue profile; Fig. 2c, blue X) in order to demonstrate the large difference in pycnocline salinity between these water sources. We define the pycnocline as 75–100 m because this depth interval falls within the upper pycnocline where the AS and AndS profiles fall on opposite ends of a relatively large salinity range. We calculate conservative temperature, absolute salinity, and sigma-density for the upper 300 m, along with the relative freshwater content (RFWC) of each measurement relative to 0.1 kg/m<sup>3</sup> density surfaces. We consider the freshest water on each density surface (RFWC = 1) to have originated from the AndS and the saltiest water (RFWC = 0) drawn from the AS.

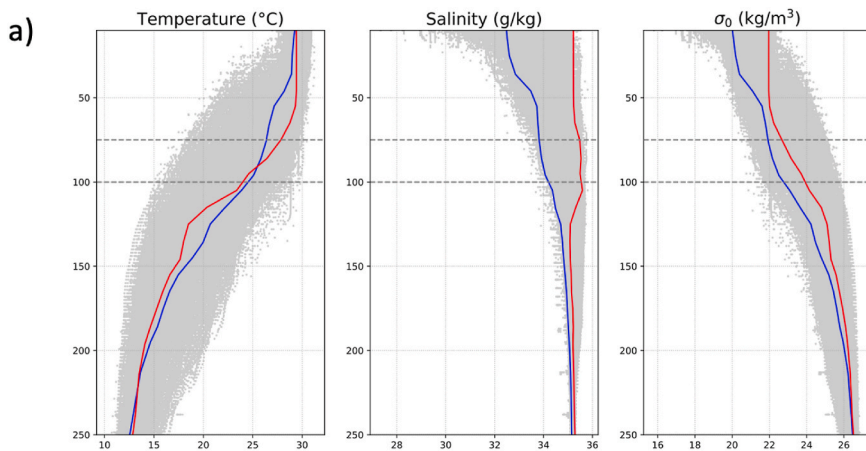


**Fig. 2.** A) Profiles, b) T-S diagram, and c) map of Argo observations in the Bay of Bengal from June–September 2004–2021. Red and blue profiles represent water from the Arabian Sea (AS) and Andaman Sea (AndS), respectively. The AS (AndS) profile location is highlighted by a red (blue) X on the map. The pycnocline is defined by the 75–100 m depth interval marked by gray dashed lines. Points in the T-S diagram (b) and map (c) are color coded for relative freshwater content (RFWC), calculated with respect to 0.1 kg/m<sup>3</sup> density surfaces. RFWC is zero for pure AS water and 1 for pure AndS water.

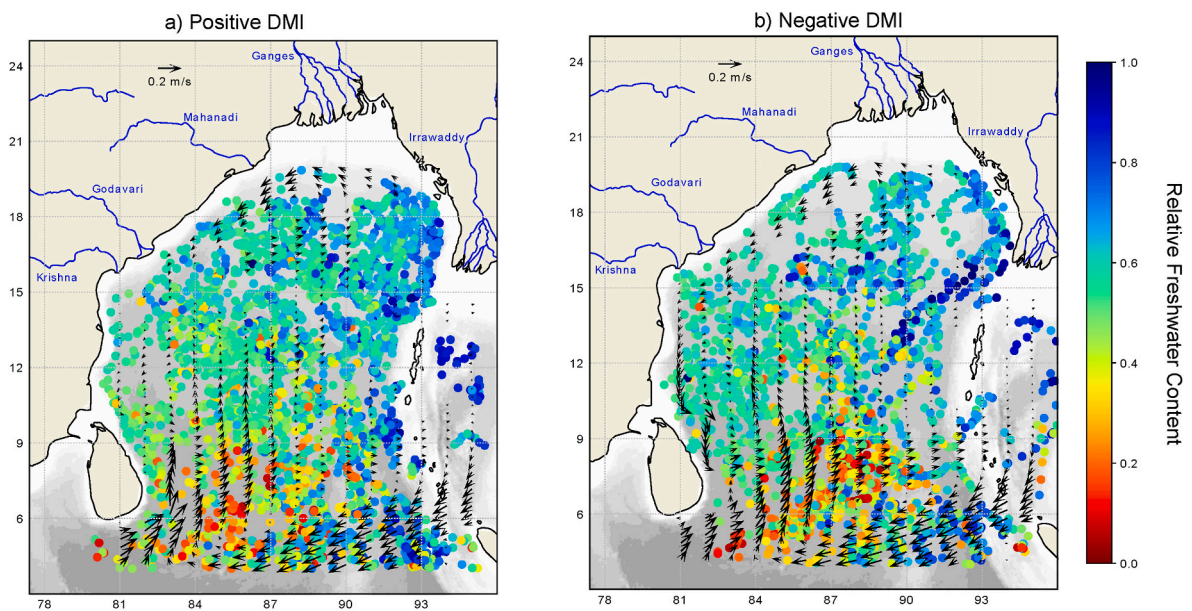
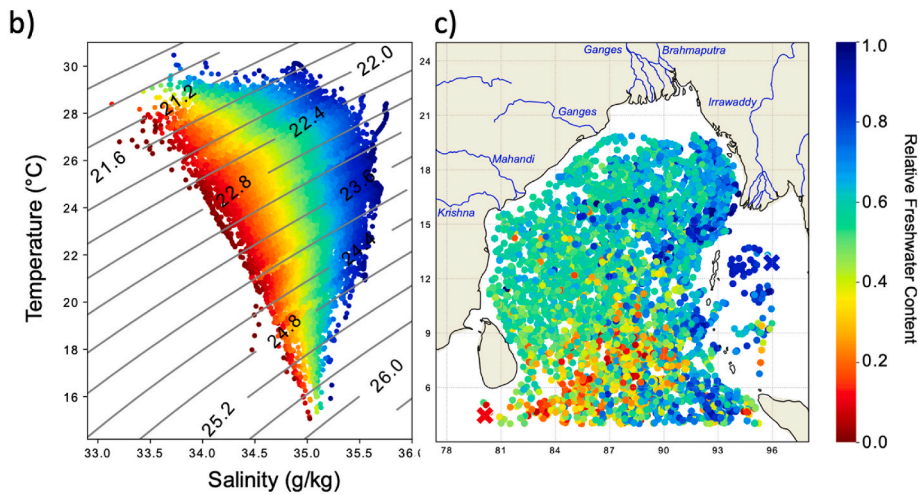


**Fig. 3.** Summer climatologies (June–September 2004–2021) of GODAS currents and Argo observations color coded for relative freshwater content (RFWC), which measures freshwater relative to 0.1 kg/m<sup>3</sup> density surfaces. RFWC is zero for pure Arabian Sea water and 1 for pure Andaman Sea water. Data is averaged over 75–100 m, for positive DMI (a) and negative DMI (b) conditions.

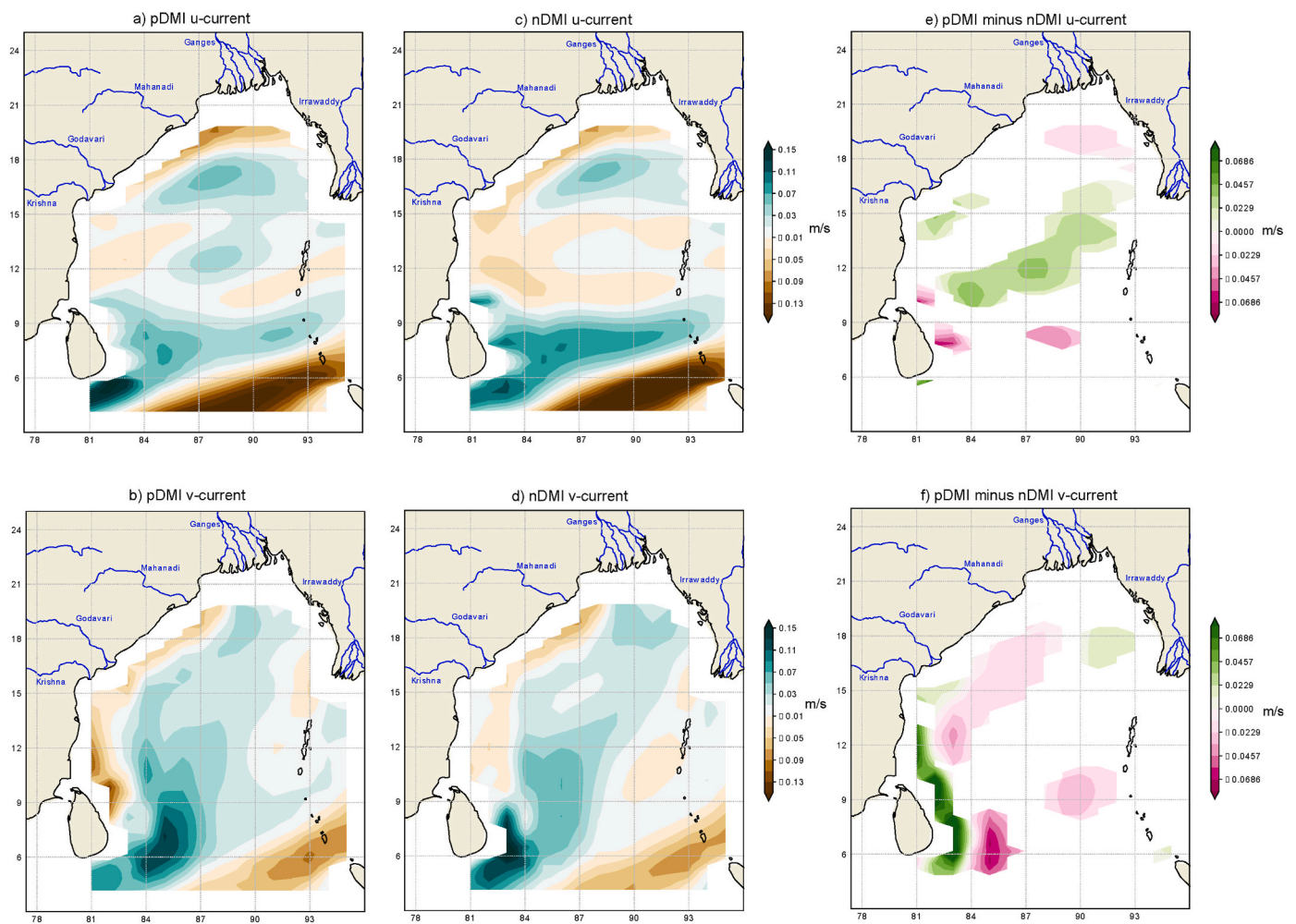


**Fig. 4.** Summer GODAS zonal (u-currents; top panel) and meridional (v-currents; bottom panel) currents averaged over 75–100 m for positive DMI (pDMI; left) and negative DMI (nDMI; middle) conditions. Regions where the difference of means between pDMI and nDMI currents are statistically significant ( $\alpha = 0.05$ ) are shown in (e) and (f).

National Centers for Environment Prediction (NCEP) Global Ocean Data Assimilation System (GODAS) is a reanalysis product that provides monthly mean subsurface currents (u and v) in 10 m intervals from 5 to 225 m (<https://www.psl.noaa.gov/data/gridded/data.godas.html>), and a spatial resolution of  $1/3 \times 1/3^\circ$  latitude and  $1 \times 1^\circ$  longitude (Behringer and Xue, 2004). GODAS has been used in several studies to study the subsurface characteristics of the IOD (Lu and Ren, 2020; Wang et al., 2020; Chen et al., 2023). In the present study, we use GODAS to relate the regional current field to the Argo freshwater spatial distribution in BoB pycnocline.

Monthly Dipole Mode Index (DMI) data is retrieved from the National Oceanic and Atmospheric Administration's Physical Sciences Laboratory ([https://psl.noaa.gov/gcos\\_wgsp/Timeseries/DMI/](https://psl.noaa.gov/gcos_wgsp/Timeseries/DMI/)). The DMI quantifies SST anomalies associated with the IOD, calculated as the difference in area-averaged monthly-mean SST deviations between the tropical western Indian Ocean ( $10^\circ\text{S}$ – $10^\circ\text{N}$ ,  $50^\circ$ – $70^\circ\text{E}$ ) and the south-eastern tropical Indian Ocean ( $10^\circ\text{S}$ –Equator,  $90^\circ$ – $100^\circ\text{E}$ ; Saji et al., 1999). SST deviation is based on linear extrapolation with respect to the 30-year sliding mean of each month. We divided our Argo and GODAS data into two groups: positive DMI (pDMI) when  $\text{DMI} > 0$ , and negative DMI (nDMI) when  $\text{DMI} < 0$ .

We use the GODAS reanalysis data to investigate whether the DMI groups differ with respect to regional velocity patterns in the BoB, which includes the Summer Monsoon Current (SMC), East India Coastal Current (EICC), and the Sri Lanka Dome (SLD). Argo RFWC is used to

evaluate the relationship between DMI and freshwater distribution. We compare the velocity patterns and freshwater distributions of the positive and negative DMI groups using a Welch's *t*-test. This test is robust against differences in variance and sample size, and it determines whether there is a significant difference in the mean values of two populations. We use a significance level of  $\alpha = 0.05$ , so a 'significant difference' indicates there is less than a 5% chance that the difference is due to random variability in the groups.

### 3. Results and discussion

There were 2111 Argo profiles recorded when  $\text{DMI} > 0$  (pDMI; Fig. 3a) and 1781 profiles recorded when  $\text{DMI} < 0$  (nDMI; Fig. 3b). In both the pDMI and nDMI summer climatologies, the strongest currents occur in anticyclonic gyre in the southern bay from  $4^\circ$  to  $9^\circ\text{N}$ . The EICC is strongest at  $20^\circ\text{N}$ , and the middle BoB is relatively quiet, likely due to the dominance of mesoscale activity in this region (Herron et al., 2022). In the nDMI map, the SMC extends farther east and there are southward currents along the east coast of Sri Lanka, while on the pDMI map these currents flow northward.

We calculated the difference in pDMI and nDMI currents at each grid point and identified regions where this difference is statistically significant. In Fig. 4e, green (purple) shading indicates there is a stronger (weaker) westward current during pDMI events. Similarly in Fig. 4f, green (purple) shading indicates there is a stronger (weaker) northward

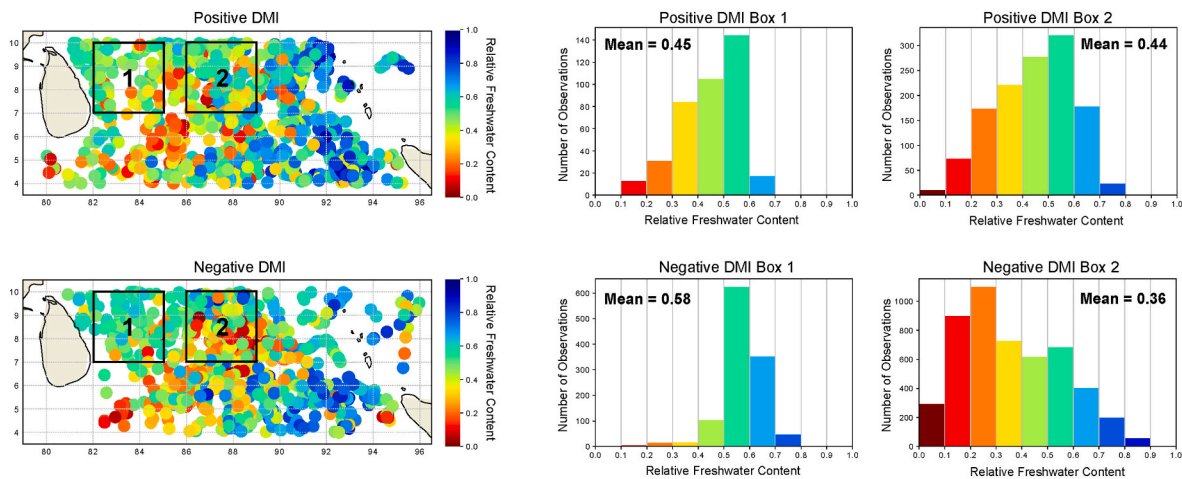


**Fig. 5.** Relative freshwater content (RFC) distribution in two boxes in the southern BoB (7–10°N) for the positive (top) and negative (bottom) DMI groups. Box 1 contains RFC values from 82 to 85°E. Box 2 contains RFC values from 86 to 89°E. Histograms show the number of observations in RFC bins of width 0.1. RFC measures freshwater relative to 0.1 kg/m<sup>3</sup> density surfaces. RFC is zero for pure Arabian Sea water and 1 for pure Andaman Sea water.

current during pDMI events. SMC, EICC, and outflow from the AndS do not show any major differences. East of Sri Lanka, the position of northward flow is shifted to the west during nDMI events.

In the southern BoB, from 4 to 10°N, freshwater increases with longitude in both the positive and negative DMI groups. However, the correlation between RFC and longitude is much stronger during pDMI ( $R = 0.45$ ;  $p = 0$ ) than it is during nDMI ( $R = 0.03$ ;  $p = 0.001$ ). We investigate the extent of AS water spreading by analyzing two  $3 \times 3^\circ$  boxes in the southern BoB from 7 to 10°N (Fig. 5). Box 1 covers the eastern portion from 82 to 84°E, and Box 2 covers the central portion from 86 to 89°E. The mean RFC in each box differs significantly between the pDMI and nDMI groups. Box 1 is saltier during pDMI conditions, but Box 2 is saltier during nDMI conditions. These differences in freshwater distribution are illustrated as histograms in Fig. 5, showing the number of Argo observations in each RFC bin of width 0.1.

#### 4. Conclusions

We combine GODAS reanalysis and Argo observational data to investigate the relationship between the IOD, quantified by DMI, and the spatial distribution of salty and fresh end members in the BoB. We find significant differences in the regional currents and freshwater distribution of the southern BoB related to the influx of AS water during positive and negative DMI events. Cullen and Shroyer (2019) attribute interannual variability of SLD position to local wind stress curl and DMI. When wind stress curl is strongly positive, as occurs during nDMI events, the SLD expands eastward, as shown in Fig. 4. RFC distribution derived from Argo data is consistent with this GODAS regional velocity pattern, as salty AS water is also shifted farther to the east during nDMI events (Fig. 5). When the SLD is more restricted to the east coast of Sri Lanka during pDMI events, AS water spreads northward closer to the east coast of Sri Lanka. While our findings support this association, further research is needed to establish a causal relationship between SLD position and the observed freshwater distributions during pDMI and nDMI conditions.

#### Availability statement

Temperature and salinity observations were collected and made freely available by the International Argo Program and the national programs that contribute to it (<https://argo.ucsd.edu>, <https://www.ocean-ops.org>). The GODAS data used for visualizing currents is available at NOAA's Physical Sciences Laboratory (<https://www.psl.noaa.gov/data/gridded/data.godas.html>).

#### Declaration of competing interest

The authors declare that they have no known competing financial interests or personal relationships that could have appeared to influence the work reported in this paper.

#### Data availability

Data will be made available on request.

#### Acknowledgements

The research was funded by Office of Naval Research, Award NO0014-22-1-2586.

#### References

- Ashok, K., Guan, Z., Saji, N.H., Yamagata, T., 2004. Individual and combined influences of ENSO and the Indian Ocean Dipole on the Indian summer monsoon. *J. Clim.* 17 (16), 3141–3155. [https://doi.org/10.1175/1520-0442\(2004\)017<3141:IACIOE>2.0.CO;2](https://doi.org/10.1175/1520-0442(2004)017<3141:IACIOE>2.0.CO;2).
- Behringer, D.W., Xue, Y., 2004. Evaluation of the global ocean data assimilation system at NCEP: the Pacific Ocean. In: Paper Presented at Eighth Symposium on Integrated Observing and Assimilation Systems for Atmosphere, Oceans, and Land Surface, AMS 84th Annual Meeting. Washington State Convention and Trade Center, Seattle, WA, pp. 11–15.
- Chatterjee, A., Shankar, D., McCreary, J., Vinayachandran, P., Mukherjee, A., 2017. Dynamics of Andaman Sea circulation and its role in connecting the equatorial Indian ocean to the bay of bengal. *J. Geophys. Res.: Oceans* 122, 3200–3218. <https://doi.org/10.1002/2016JC012300>.
- Chen, G., Han, W., Ma, X., Li, Y., Zhang, T., Wang, D., 2023. Role of extreme Indian Ocean Dipole in regulating three-dimensional freshwater content in the Southeast Indian Ocean. *Geophys. Res. Lett.* 50, e2022GL102290 <https://doi.org/10.1029/2022GL102290>.
- Cullen, K., Shroyer, E., 2019. Seasonality and interannual variability of the Sri Lanka Dome. *Deep Sea Res. Part II: special issue on the Bay of Bengal* 168. <https://doi.org/10.1016/j.dsr2.2019.104642>.
- Gordon, A.L., Shroyer, E.L., Mahadevan, A., Sengupta, D., Freilich, M., 2016. Bay of Bengal: 2013 northeast monsoon upper-ocean circulation. *Oceanography* 29 (2), 82–91. <https://doi.org/10.5670/oceanog.2016.41>.
- Gordon, A.L., Shroyer, E.L., Fernando, H.J.S., Tandon, A., Mathur, M., Priyantha Jinadasa, S.U., 2019. Introduction to "Atmosphere-Ocean Dynamics of Bay of Bengal" Volume 1, Deep-Sea Research Part II. <https://doi.org/10.1016/j.dsr2.2019.104670>.
- Herron, A.J., Bohman, S.M., Gordon, A.L., 2022. Freshwater transport by eddies within the Bay of Bengal's central axis. *Deep-Sea Res. Part I* <https://doi.org/10.1016/j.dsr.2022.103770>.
- Hormann, V., Centurioni, L., Gordon, A.L., 2019. Freshwater export pathways from the bay of bengal. In: Deep Sea Research II, Special Issue on the Bay of Bengal. <https://doi.org/10.1016/j.dsr2.2019.104645>.
- Jampana, V., Ravichandran, M., Kantha, Lakshmi, Rahaman, Hasibur, 2019. Modeling slippery layers in the northern Bay of Bengal. *Deep Sea Res. Part II Top. Stud. Oceanogr.* 168 <https://doi.org/10.1016/j.dsr2.2019.07.004>.

- Jithin, A.K., Francis, P.A., Unnikrishnan, A.S., Ramakrishna, S.S.V.S., 2020. Energetics and spatio-temporal variability of semidiurnal internal tides in the Bay of Bengal and Andaman Sea. *Prog. Oceanogr.* 189, 102444 <https://doi.org/10.1016/j.pocean.2020.102444>. ISSN 0079-6611.
- Lu, B., Ren, H.-L., 2020. What caused the extreme Indian Ocean Dipole event in 2019? *Geophys. Res. Lett.* 47, e2020GL087768 <https://doi.org/10.1029/2020GL087768>.
- McKenna, S., Santoso, A., Sen Gupta, A., Taschetto, A.S., Cai, W., 2020. Indian Ocean Dipole in CMIP5 and CMIP6: characteristics, biases, and links to ENSO. *Nature: Sci. Rep.* 19, 11500 <https://doi.org/10.1038/s41598-020-68268-9>.
- Meyers, G., McIntosh, P., Pigot, L., Pook, M., 2007. The years of El Niño, La niña, and interactions with the tropical Indian ocean. *J. Clim.* 20 (13), 2872–2880. <https://doi.org/10.1175/JCLI4152.1>.
- Osborne, A.R., Burch, T.L., 1980. Internal solitons in the Andaman Sea. *Science* 208, 451–460. <https://doi.org/10.1126/science.208.4443.451>.
- Saji, N.H., Goswami, B.N., Vinayachandran, P.N., Yamagata, T., 1999. A dipole mode in the tropical Indian Ocean. *Nature* 401, 360–363.
- Varkey, M.J., Murty, V.S.N., Suryanarayana, A., 1996. Physical oceanography of the bay of bengal and Andaman Sea. *Oceanogr. Mar. Biol. Annu. Rev.* 34, 1–70.
- Wang, G., Cai, W., Yang, K., Santoso, A., Yamagata, T., 2020. A unique feature of the 2019 extreme positive Indian Ocean Dipole event. *Geophys. Res. Lett.* 47, e2020GL088615 <https://doi.org/10.1029/2020GL088615>.
- Wibowo, M.A., Tanjung, A., Rifardi, Elizal, Mubarak, Yoswaty, D., Susanti, R., Muttaqin, A.S., Fajary, F.R., Anwika, Y.M., 2022. Understanding the mechanism of currents through the Malacca Strait study case 2020 – 2022 : mean state, seasonal and monthly variation. *IOP Conf. Ser. Earth Environ. Sci.* 1118, 012069 <https://doi.org/10.1088/1755-1315/1118/1/012069>.
- Wong, A., Wijffels, S.P., Riser, S.E., Pouliquen, S.C., Hosoda, S., Roemmich, D., et al., 2020. Argo data 1999–2019: two million temperature-salinity profiles and subsurface velocity observations from a global array of profiling floats. *Front. Mar. Sci.* 7 <https://doi.org/10.3389/fmars.2020.00700>.
- Wyrtki, K., 1961. *Physical Oceanography of the Southeast Asian Waters*. Scripps Institution of Oceanography, UC San Diego.